

CALORIMETRIC DATA FOR α -AlMnSi AND THE α -TO- β DECOMPOSITION

K. REDFORD and J.E. TIBBALLS

Senter for Industriforskning, PB 124 Blindern, N-0314 Oslo 3 (Norway)

R. McPHERSON

Department of Materials Engineering, Monash University, Clayton, Victoria 3168 (Australia)

(Date received 10 July 1989)

ABSTRACT

The specific heat of α -AlMnSi crystals precipitated from liquid solutions and separated by dissolution of the aluminium solid solution has been determined as $C_p = 21.06 + 0.00917T$ J mol⁻¹ K⁻¹. The heat of decomposition at 1027 K to a liquid plus β -Al₉Mn₃Si was measured as 3200 ± 200 J mol⁻¹. The reaction products of the α -phase with highest Si content (11.8 wt.% Si) are a liquid of composition Al–7 wt.% Mn–14 wt.% Si and β -AlMnSi with 36.5 wt.% Mn and 11.6 wt.% Si. The phase diagram for Al–Mn–Si has been extended to 18 wt.% Si and 40 wt.% Mn. The extra Si atoms in the β -phase are assigned to the 6-fold sublattice occupied otherwise by aluminium.

INTRODUCTION

The α -phase of the AlMnSi ternary alloy system is an important component of many aluminium and magnesium alloys. Its crystal structure possesses features that suggest a close resemblance to the quasi-crystalline I-phases [1]. Indeed, the I-phase is a precursor of the α -phase in the sequence of solid-state precipitation reactions in strip-cast, high-Mn aluminium alloys [2]. The need to understand the role of Si in stabilizing the α -phase motivated a recent study [3] of Al–Si substitution in the crystal structure.

In order to establish the Gibbs free energy of the phase as a function of composition and temperature, data are required on the specific heat and enthalpies of reaction as well as the nature of the equilibria into which the phase enters.

The specific heat of α -AlMnSi has been measured [4] for temperatures up to 30 K. The Debye temperature of 425 K derived from these results is sufficiently high to suggest that the specific heat will increase significantly over the temperature range of interest for aluminium and magnesium metallurgy.

Phillips' phase diagrams [5] for the AlMnSi system indicate that the reaction



occurs from temperatures below 660 °C, for total Si concentrations less than 4 wt.%, to above 740 °C, for concentrations greater than 9 wt.% Si.

In this study, we present measurements of the specific heat of α -AlMnSi up to 900 K [625 °C], the temperature and enthalpy of decomposition reaction (1) and the compositions of the reactants. X-ray powder diffraction data for the β -AlMnSi resulting from reaction (1) enable the model of Al–Si substitution derived for that phase in [3] to be extended to higher Si concentrations. The experimental liquidus surface can also be extended and the temperature determined for the eutectic between silicon, the aluminium solid solution and the metastable β -phase.

MATERIALS AND TECHNIQUES

The preparation of the α -AlMnSi samples has been described previously [3]. Their compositions are given in Table 1. All four samples were investigated by differential thermal analysis (DTA). Sample 4 was chosen for specific heat measurements because its X-ray powder diffraction pattern showed no detectable contamination by silicon or the aluminium solid solution.

To obtain the decomposition products of reaction (1), specimens of sample 5 were held in the DTA furnace at 800 °C for 2 h, then air-quenched. The time to reach 400 °C was ~ 20 s. The products consisted of a single solidified droplet, 0.7 mm in diameter, and a number of 0.2-mm grains. The droplet was analysed electron-optically, the grains by means of X-ray diffraction.

DTA was performed on lightly crushed, ca. 5 mg specimens in a Rigaku high-temperature micro DTA apparatus by heating to 960 °C at 2.5 °C

TABLE 1

Composition of α -AlMnSi specimens extracted from castings. Microprobe analyses supplemented by wet analysis; standard deviations in parentheses

Casting no.	Composition (wt.%)		
	Al	Mn	Si
2	61.0(5)	29.2(4)	9.8(3)
3	60.0(4)	29.5(2)	10.5(3)
4	59.1(4)	29.6(2)	11.3(3)
5	58.5(5)	29.7(5)	11.8(3)

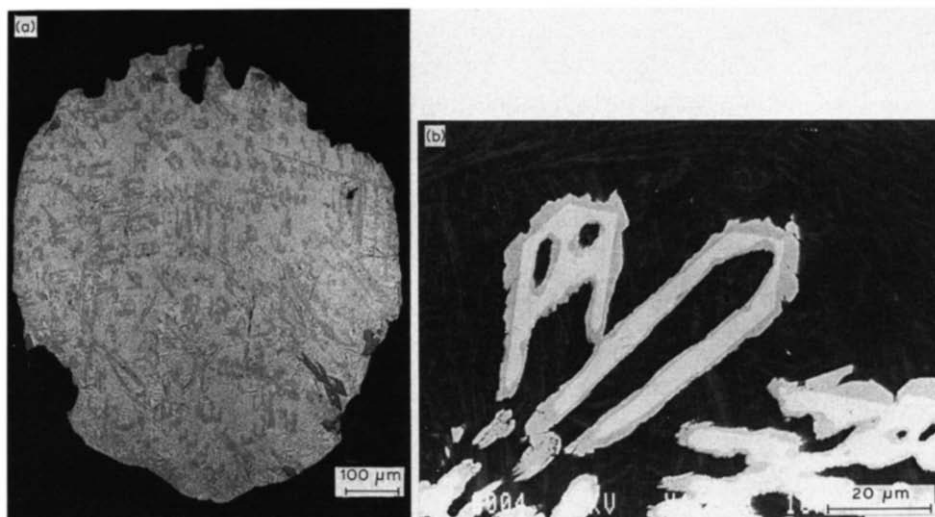


Fig. 1. (a) Section of droplet formed by air-quenching sample 5 from 800 °C; (b) back-scattered electron image of precipitates in the solidified droplet. The phases in order of increasing lightness are the α -Al solid solution, Si needles, and α -AlMnSi growing peritectically around the lightest phase, β -AlMnSi.

min^{-1} . The reference material was powdered Al_2O_3 and argon was used as the dynamic shielding gas. Alumina specimen pans were used. The instrument was calibrated with a sample of 99.99% aluminium for which the specific heat was taken as $(20.62 + 0.01246T) \text{ J mol}^{-1} \text{ K}^{-1}$ and the enthalpy of fusion at 660 °C was $10.67 \text{ kJ mol}^{-1}$ [6]. The data were analysed by standard methods [7] to give an accuracy of 5% in enthalpy and 10% in specific heat.

A specimen of the air-quenched reaction products was reheated at $20^\circ \text{C min}^{-1}$ to observe the temperatures of reactions between the products.

Differential scanning calorimetry was employed to determine the temperature dependence of the heat capacity. Data were obtained by analysing the heat flux over the temperature range 25–625 °C. The calorimeter used was a Perkin–Elmer DSC-7 with alumina sample pans. Argon was used as the dynamic shielding gas. Calibration was performed with 99.999% indium with a melting temperature of 156.6 °C (429.8 K) and ΔH_f 28.45 J mol^{-1} and with 99.998% zinc with a melting temperature of 419.5 °C (692.7 K).

Quantitative electron-optic analyses of the droplet from an air-quenched specimen of sample 5 were undertaken to establish the compositions of the reaction products. In back-scattered electron images (b.e.i.) obtained from a polished section in a CAMECA CAMEBAX electron microprobe (see Fig. 1), the four phases α - and β -AlMnSi, Si and the α -Al solid solution could be distinguished by their grey tone. Each phase was analysed for Al, Mn and Si by wavelength-dispersive spectroscopic (WDS) methods. The fineness of the

α -Al + Si mixture precluded analysis of the individual phases, so area analyses were employed to establish the average composition.

The b.e.i. obtained in a JEOL scanning electron microscope were transferred to a KONTRON IBAS analyser and the area fractions of each phase were measured. These were combined with data on phase densities in order to determine the weight fraction of each phase.

X-ray powder diffraction was undertaken on the granular component of the air-quenched specimen from sample 5. The lattice parameters were determined for the dominant phase, hexagonal β -AlMnSi.

RESULTS

The DTA curves obtained on heating each sample are shown in Fig. 2. In addition, the cooling curve for sample 3 illustrates the thermal inertia in the instrument. The endothermic peak for the fusion of aluminium was used to calibrate both temperature and enthalpy data. The endothermic reaction at 1027 ± 3 K with an enthalpy of $3200 (\pm 200)$ J mol⁻¹ is that shown in eqn. (1). The final dissolution of β -AlMnSi in the liquid alloy occurs at 1225 K. For sample 5, a second, exothermic reaction occurs at temperatures above 1130 K.

Reheating of air-quenched samples gave a double peak (see Fig. 2) below 900 K. The upper peak, readily identified as the equilibrium eutectic, is at 846 K, the second peak being 10–15 K lower in temperature.

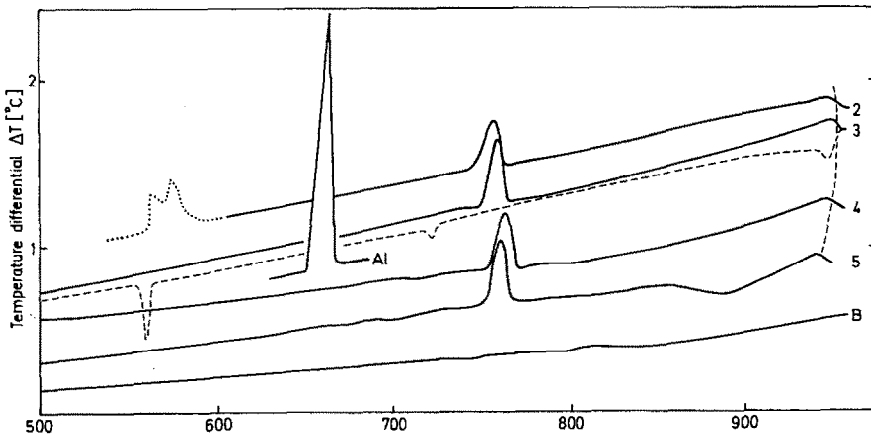


Fig. 2. DTA curves for samples 2–5 heated at $2.5^\circ\text{C min}^{-1}$. The peak from melting the 0.0822 g, 99.99% Al calibration sample is also shown. The dotted double peak represents the additional feature found on reheating air-quenched specimens. The background (B) or empty-can trace is drawn correctly relative to the trace for sample 5. The trace obtained on cooling sample 3 at the same rate (dashed line) indicates the thermal inertia in the instrument.

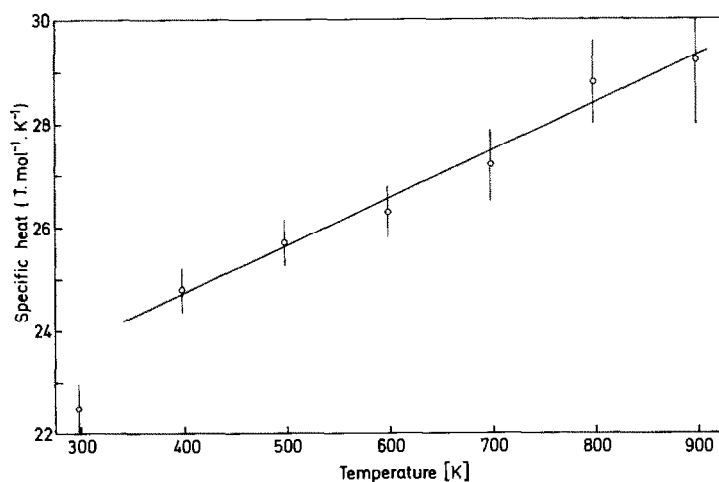


Fig. 3. Specific heat of α -AlMnSi over the temperature range 298–898 K. The straight line represents the equation $C_p = 21.06 + 0.0091T \text{ J mol}^{-1} \text{ K}^{-1}$.

Analysis of the DTA curves for Al and the α -phase from room temperature to 600 K gave an estimate for the specific heat of α -AlMnSi as $25(3) \text{ J mol}^{-1} \text{ K}^{-1}$. This proved to be in excellent agreement with the specific heat measured by differential scanning calorimetry, as shown in Fig. 3.

The metallographic analyses of the air-quenched droplet enabled the weight fractions of each of the phases and their compositions to be established, as shown in Table 2.

The X-ray powder diffraction pattern showed lines from the α -Al solid solution, α - and β -AlMnSi and Si. The relative heights of the strongest reflections for each were as follows

$$\alpha\text{-Al}(111) : \alpha\text{-AlMnSi}(532) : \beta\text{-AlMnSi}(301) : \text{Si}(1) = 35 : 18 : 100 : 10$$

The lattice parameters for β -AlMnSi, determined by refining d -spacings for reflections out to 420, were $a = 0.7476 \text{ nm}$ and $c = 0.7687 \text{ nm}$.

TABLE 2

Compositions and fractions of phases in the air-quenched droplet. The composition of the liquid phase is estimated as the mass-weighted sum of the α -Al, Si and α -AlMnSi phases

Phase	Area ^a (%)	Mass (%)	Composition (wt.%)			Density (g cm ⁻³)
			Al	Mn	Si	
α -Al	53.7 (1.7)	48.5	—	—	—	2.7
Si	11.1 (0.9)	8.5	0	0	100	2.3
α -Al + Si	64.8 (1.9)	57.0	79.8	0.45	19.75	—
α -AlMnSi	14.6 (1.5)	17.3	58.2	28.4	13.4	3.55
Liquid	—	74.3	75	7	18	—
β -AlMnSi	20.6 (1.0)	25.7	51.4	37.0	11.6	3.74

^a Standard deviation given in parentheses.

DISCUSSION

The DTA curves for the heating of samples 1–4 are virtually identical with the endothermic peak for decomposition reaction (1) at 1027 ± 3 K having enthalpy of reaction of 3200 ± 200 J mol⁻¹. The liquidus temperature for the peritectic dissolution of β -AlMnSi, as measured by the point of inflection, was 1223 ± 3 K for all sample compositions. This temperature coincides closely with the liquidus temperature for 29 wt.% Mn in the Al–Mn binary system.

The exothermic reaction observed for sample 5 above 1130 K is presumed to result from the dissolution of Si in the liquid + β -AlMnSi mixture. Free Si was present in this specimen because it is not dissolved by the hot butanol employed to extract the α -phase from the Al solid solution [3].

The portion of the specimen examined metallographically after quenching from 1075 K contained fragments of free Si in addition to the Si needles that formed on solidification. At this temperature, the liquid had clearly accumulated to a droplet containing some β -phase, leaving several grains of the β -phase with little of the melt surrounding them. The total Mn analysis of the droplet was much lower than that of sample 5. The predominance of β -AlMnSi lines in the X-ray pattern, which was taken from the granular portion, confirms this accumulation.

The lower of the double peaks at 846 and 834 K observed in DTA (Fig. 2) on reheating quenched samples can be attributed to the metastable eutectic between β -AlMnSi, Si and the saturated liquid solution.

The composition of the liquid entering into this metastable equilibrium has not been determined. The composition of the liquid from which the Si needles precipitate was approximately 20 wt.% Si, 0.4 wt.% Mn. Clearly, however, the needles have grown rapidly into the melt, indicating that this value is well above the Si concentration of the metastable eutectic.

The analysis of the β -phase formed at 1027 K is straightforward with electron-optic and WDS techniques. The composition of the coexisting liquid, however, had to be estimated from a knowledge of the volume fraction and composition of each phase. It is seen in Fig. 1, for the droplet formed in the air-quenched specimen, that the α -phase has formed a 1- μ m thick peritectic layer around each β -phase particle in the period of ~ 10 s that was available as the temperature fell from 1027 to 846 K. This time has been sufficient to drain virtually all Mn from liquid solution (the Mn content of the α -Al + Si mixture after solidification is only 0.4 wt.%). This agrees with measured Mn diffusivities at 700 and 800 °C of 0.7×10^{-6} and 1.5×10^{-6} cm² s⁻¹ [8]. Furthermore, it indicates that the liquid would be able to maintain its equilibrium concentration of Mn with respect to β -AlMnSi at these cooling rates. The composition of the liquid at the α - β transition temperature can therefore be estimated as the sum of the compositions of the α -AlMnSi, α -Al solid solution and Si given in Table 2. The

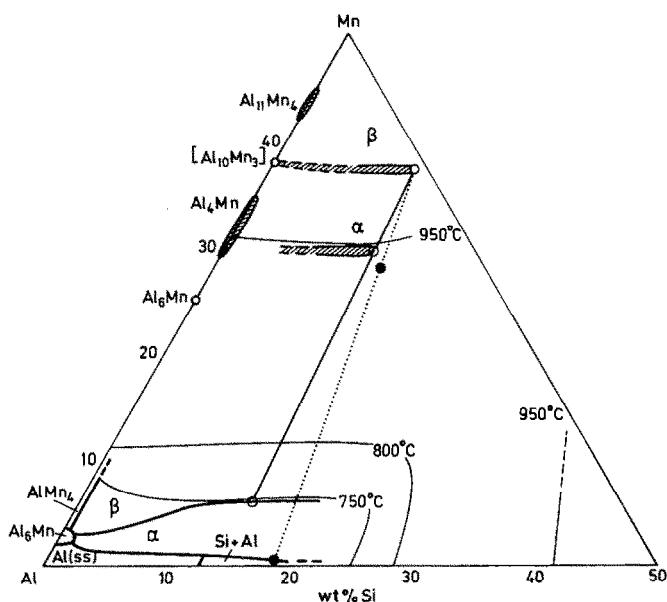
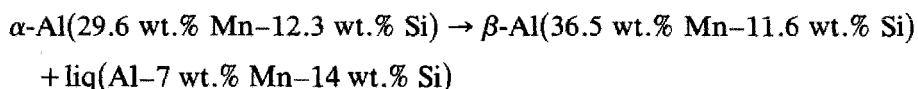


Fig. 4. The phase diagram from ref. 5 extended to 35 wt.% Mn and 20 wt.% Si on the basis of the present observations. Open circles represent compositions of the phases in equilibrium at 1027 °C in sample 5, whereas the filled circles are the compositions of the α -phase and liquid formed on air-quenching sample 5 from 1075 K. The compositions of the binary and ternary phases are indicated and the boundaries of the liquidus surfaces drawn. The temperature contours for the liquidus surfaces are extended from the binaries to account for the present data.

complete specification of the observed decomposition reaction is



Phillips' liquidus surface [5] shows the boundary between α - and β -AlMnSi on the basis of measurements up to approximately 10 wt.% Si. He surmised a continuation to higher Mn and Si concentrations at higher temperatures, but it is clear from the data presented here that 7 wt.% Mn and 1027 K represent upper values for the primary precipitation of α -phase at high Si concentrations. The extended phase diagram is shown in Fig. 4 with isotherms sketched from the binary liquidus.

We note that the Mn concentration in the α -phase that precipitated peritectically during quenching represents a deficiency of approximately 1.5 (of 24) Mn atoms per unit cell compared with the ideal crystal structure. The concentration of silicon in the phase represents almost 21 atoms per unit cell.

As Fig. 3 shows, the specific heat of α -AlMnSi can be described by

$$C_p = 21.062 + 0.0091T \quad \text{J mol}^{-1} \text{K}^{-1}$$

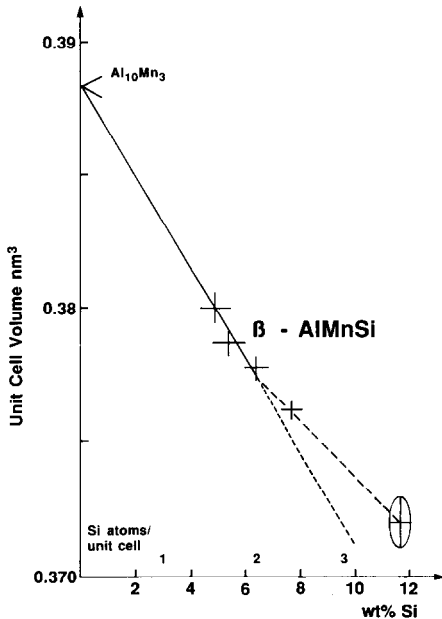


Fig. 5. The relationship between unit cell volume and Si content for β -AlMnSi from [3] extended to 12 wt.% Si. Data for $\text{Al}_{10}\text{Mn}_3$ ($<$), β -AlMnSi from [9] ($+$) and the present result (ellipse). Note the change in slope at 2 Si atoms per unit cell as atoms begin to substitute on to the $6(h)$ sites rather than the $2(d)$ sites.

for the temperature range $T = 375\text{--}875$ K. This is similar to the value for Al, but somewhat lower than that for Mn, for which $C_p = 21.75 \pm 0.0165 T \text{ J mol}^{-1} \text{ K}^{-1}$ [6].

The X-ray diffraction spectra from the air-quenched granules were dominated by lines for hexagonal β -AlMnSi with a small unit cell. As seen in Fig. 5, the cell volume for 11.6 wt.% Si, 372 \AA^3 , is nonetheless larger than expected from the extrapolation of the data for volume versus Si content presented in [3]. Given, however, that the present composition represents 3.6 Si atoms per unit cell, it is clear that a second sublattice of atomic positions in addition to the $2(d)$ positions must now be occupied by Si atoms (See ref. 9 for details of the β -phase crystal structure). Of the remaining Al sites, Wyckoff positions $6(h)$ and $12(k)$, and the vacant $2(d)$ site, the $6(h)$ site seems most likely as (a) no Si nearest neighbour pairs need be created until half the sites are filled, and (b) it has short bonds to two Mn atoms. These features, plus the fact that the change in unit cell volume between 2 and 3.6 Si atoms per unit cell is 3.7 \AA^3 per Si atom substituted, suggest a similarity between $6(h)$ and the Al(3) site in α -AlMnSi. The Al(3) site has an irregular icosahedral coordination shell with 2 Mn atoms; the coordination of the $6(h)$ sites in β -AlMnSi is similar in both respects. To avoid Si nearest neighbours among the $6(h)$ sites in this crystal structure, the number of Si atoms must not exceed three and hence the number of Si atoms per unit cell

must remain less than five. This places a likely upper stability limit on the Si content of 19 wt.%.

CONCLUSIONS

DTA and quantitative electron-optic metallography have shown that the phase α -AlMnSi with Si concentrations greater than 9 wt.% decomposes to the phase β -AlMnSi plus a liquid solution at 1027 K in an endothermic reaction requiring 3200 J mol^{-1} . The specific heat has furthermore been determined over the range 375–875 K as $20.385 + 0.0099T \text{ J mol}^{-1} \text{ K}^{-1}$. One pair of coexisting compositions at 1027 K for the liquid solution and β -AlMnSi has been determined as 7 wt.% Mn–14 wt.% Si and 36.5 wt.% Mn–11.6 wt.% Si, respectively. The unit cell volume at this high Si content suggests that above 2 atoms per unit cell Si substitutes for Al on the $6(h)$ lattice position rather than the $2(d)$ position found previously for compositions up to 2 atoms per unit cell.

ACKNOWLEDGEMENTS

This work has been funded by the Royal Norwegian Council for Scientific and Industrial Research (NTNF) under grant MT10.23822 and supported by Hydro Aluminium AS and Elkem Aluminium AS. The assistance of our colleagues Rolf Kalland (sample preparation), Trond Wahl (metallography), Jens-Anton Horst (WDS analysis), Kari Baardseth (SEM) and Trine-Lise Rolfsen (X-ray diffraction) is gratefully acknowledged.

REFERENCES

- 1 P. Guyot and M. Audier, *Philos. Mag.*, B, 52 (1985) L15.
- 2 V. Hansen, J. Gjønnes and B. Andersson, *J. Mater. Sci. Lett.*, 8 (1989) 823.
- 3 J.E. Tibballs, R.L. Davis and B.A. Parker, *J. Mater. Sci.*, 24 (1989) 2177.
- 4 M. Masner, J. van der Berg and J.A. Mydosh, *Europhys. Lett.*, 3 (10) (1987) 1103.
- 5 H.W.L. Phillips, *J. Inst. Met.*, 69 (1943) 275.
- 6 O. Kubachewski and C.B. Alcock, *Metallurgical Thermochemistry*, 5th edn., Pergamon, Oxford, 1979.
- 7 D.T. David, *Anal. Chem.*, 36(11) (1964) 2162.
- 8 G.S. Ershov, A.A. Kasatkin and A.A. Golubev, *Izv. Akad. Nauk SSSR, Met.*, (2) (1979) 77.
- 9 K. Robinson, *Acta Crystallogr.*, 5 (1952) 397.